

UC Irvine

UC Irvine Previously Published Works

Title

The Novel Desmin Mutant p.A120D Impairs Filament Formation, Prevents Intercalated Disk Localization, and Causes Sudden Cardiac Death

Permalink

<https://escholarship.org/uc/item/9hq8v0w1>

Journal

Circulation Genomic and Precision Medicine, 6(6)

ISSN

1942-325X

Authors

Brodehl, Andreas
Dieding, Mareike
Klauke, Bärbel
[et al.](#)

Publication Date

2013-12-01

DOI

10.1161/circgenetics.113.000103

Copyright Information

This work is made available under the terms of a Creative Commons Attribution License, available at <https://creativecommons.org/licenses/by/4.0/>

Peer reviewed

The Novel Desmin Mutant p.A120D Impairs Filament Formation, Prevents Intercalated Disk Localization, and Causes Sudden Cardiac Death

Andreas Brodehl, PhD*; Mareike Dieding, MSc*; Bärbel Klauke, PhD; Eric Dec, MD; Shrestha Madaan, MD; Taosheng Huang, MD, PhD; John Gargus, MD, PhD; Azra Fatima, PhD; Tomo Šarić, MD, PhD; Hamdin Cakar, PhD; Volker Walhorn, PhD; Katja Tönsing, PhD; Tim Skrzypczyk, MSc; Ramona Cebulla, TN; Désirée Gerdes, TN; Uwe Schulz, MD; Jan Gummert, MD; Jesper Hastrup Svendsen, MD, DMSc; Morten Salling Olesen, PhD; Dario Anselmetti, PhD; Alex Hørby Christensen, MD, PhD; Virginia Kimonis, MD; Hendrik Milting, PhD

Background—The intermediate filament protein desmin is encoded by the gene *DES* and contributes to the mechanical stabilization of the striated muscle sarcomere and cell contacts within the cardiac intercalated disk. *DES* mutations cause severe skeletal and cardiac muscle diseases with heterogeneous phenotypes. Recently, *DES* mutations were also found in patients with arrhythmogenic right ventricular cardiomyopathy. Currently, the cellular and molecular pathomechanisms of the *DES* mutations leading to this disease are not exactly known.

Methods and Results—We identified the 2 novel variants *DES*-p.A120D (c.359C>A) and *DES*-p.H326R (c.977A>G), which were characterized by cell culture experiments and atomic force microscopy. Family analysis indicated a broad spectrum of cardiomyopathies with a striking frequency of arrhythmias and sudden cardiac deaths. The in vitro experiments of desmin-p.A120D reveal a severe intrinsic filament formation defect causing cytoplasmic aggregates in cell lines and of the isolated recombinant protein. Model variants of codon 120 indicated that ionic interactions contribute to this filament formation defect. Ex vivo analysis of ventricular tissue slices revealed a loss of desmin staining within the intercalated disk and severe cytoplasmic aggregate formation, whereas z-band localization was not affected. The functional experiments of desmin-p.H326R did not demonstrate any differences from wild type.

Conclusions—Because of the functional in vivo and in vitro characterization, *DES*-p.A120D has to be regarded as a pathogenic mutation and *DES*-p.H326R as a rare variant with unknown significance. Presumably, the loss of the desmin-p.A120D filament localization at the intercalated disk explains its clinical arrhythmogenic potential. (*Circ Cardiovasc Genet.* 2013;6:615-623.)

Key Words: arrhythmias, cardiac ■ cardiomyopathies ■ death, sudden ■ desmin ■ desmosomes ■ intermediate filaments

The intermediate filament (IF) protein desmin is encoded by the gene *DES* and contributes to the mechanical stabilization of the sarcomeres and cell contacts within the cardiac intercalated disk (ID). Desmin is the predominant IF protein of striated muscles. It belongs to the type III IF proteins characterized by a uniform assembly mechanism. In the first step of the in vitro assembly, 2 coiled-coil dimers form an antiparallel tetramer.¹ These tetramers are the essential building blocks of the IF. Eight tetramers anneal in lateral orientation into unit length filaments. In the longitudinal elongation step, these unit length filaments are assembled and radially compacted

into IF.² Since the first reports on *DES* mutations,³⁻⁵ it became obvious that *DES* mutations cause skeletal myopathies and different forms of cardiomyopathies.^{6,7}

Clinical Perspective on p 623

In the meantime, >60 different *DES* mutations distributed over the whole sequence are known, which lead to filament formation defects with deposition of cytoplasmic desmin aggregates in the majority of cases.^{8,9} However, the pathomechanisms of desmin aggregation leading to skeletal or cardiac myopathies are mechanistically not understood in detail. Moreover,

Received February 8, 2013; accepted October 12, 2013.

The current address for Dr Brodehl is Department of Cardiac Sciences, Libin Cardiovascular Institute of Alberta, University of Calgary, Calgary, Alberta, Canada.

*Dr Brodehl and M. Dieding contributed equally to this work.

The online-only Data Supplement is available at <http://circgenetics.ahajournals.org/lookup/suppl/doi:10.1161/CIRCGENETICS.113.000103/-DC1>.

Correspondence to Andreas Brodehl, PhD, Department of Cardiac Sciences, Libin Cardiovascular Institute of Alberta, University of Calgary, 3280 Hospital Dr NW, T2N4Z6 Calgary, Alberta, Canada. E-mail abrodehl@ucalgary.ca or Hendrik Milting, PhD, Erich and Hanna Klessmann Institute for Cardiovascular Research and Development (EHKI), Heart and Diabetes Center NRW, Ruhr-University Bochum, D-32545 Bad Oeynhausen, Germany. E-mail hmilting@hdz-nrw.de

© 2013 American Heart Association, Inc.

Circ Cardiovasc Genet is available at <http://circgenetics.ahajournals.org>

DOI: DOI: 10.1161/CIRCGENETICS.113.000103

aggregate formation of mutant desmins does not explain per se the arrhythmogenic phenotype of some cardiomyopathies.

Recently, different *DES* mutations were also identified in patients with arrhythmogenic right ventricular cardiomyopathy (ARVC).^{10–15} ARVC is an inherited cardiomyopathy clinically characterized by arrhythmias and predominately right ventricular dilatation leading to cardiac syncope, heart failure, or even sudden cardiac death (SCD).¹⁶ It is well established that mutations in the genes coding for desmosomal plaque proteins cause ARVC^{17–19} and rare forms of dilated cardiomyopathy.²⁰ In the cardiac muscle, desmin is found in costamers, the z-disk, and connected via plaque proteins to the cardiac desmosome within the ID. The molecular processes contributing to the destabilization of the ID through desmin filaments are fragmentarily understood. Especially, it is not known, how and which of the desmin mutations impair the connection of the IF system to the cardiac desmosome.

In this study, we report a novel pathogenic *DES* mutation (c.359C>A, p.A120D), which seems to interfere particularly with the connection of desmin IF to the ID. Furthermore, we investigate whether the *DES* variants p.A120D and p.H326R (c.977A>G) affect the IF formation using ectopic expression cell culture systems and atomic force microscopy (AFM). These data reveal that desmin-p.A120D but not desmin-p.H326R inhibits the longitudinal assembly step, confirming its pathogenic potential.

Materials and Methods

Clinical Description of the Patients

In family A, the 34-year-old female index patient (III:24) presented with atrial flutter, variable atrioventricular conduction (Figure I in the online-only Data Supplement), and dilated atria. The average ventricular frequency was 64 bpm, and the atrial frequency was 120 bpm. In the ECG, some polymorphic premature ventricular contractions (PVCs) with a frequency of 45 to 111 bpm were detected (Figure I in the online-only Data Supplement). The cardiological evaluation including 2-dimensional, M-mode, spectral, and color Doppler was performed. These investigations reveal normal left ventricular (LV) systolic function (LV ejection fraction of 67%), a borderline concentric LV hypertrophy. Nevertheless, the left atrium was severely dilated and the right atrium was also dilated. She is a member of a large family with dilated cardiomyopathy and several SCDs (Figure 1A). The patient had no signs of a myopathy but received an implantable cardioverter defibrillator. She had 1 sister (III:21) and 2 brothers (III:22, III:23) who died from SCD as teenagers (aged 13, 17, and 13 years, respectively). Her father (II:13) and grandfather (I:3) died because of cardiomyopathy at the age of 33 and 45 years, respectively. Patient III:24 lost 3 aunts (II:2 aged 34 years, II:4 aged 42 years, and II:10 aged 50 years) by SCD. Another 4 members of family A died suddenly at the age of 13 (III:3, III:4, III:15) and 30 years (III:16). One paternal aunt (II:6) of the index patient (III:24) who had Ebstein anomaly was transplanted. All children of II:6 were without cardiac disease. The index patient (III:24) and her aunt (II:6) were heterozygous for the *DES* mutation p.A120D (c.359C>A). Her son (IV:3) had the wild-type (WT) alleles of the *DES* gene and presented no signs of a muscle disease. The mutation was not found in the children of patient II:6. One cousin of the index patient (III:7) was positive for the *DES* mutation p.A120D. The ECG of patient (III:7) showed normal sinus rhythm with prolonged PR interval, T-wave abnormalities, and AV block. Furthermore, patient III:7 was examined by echocardiography and MRI. The patient revealed normal LV size and normal LV systolic function (LV ejection fraction 64% by biplane). There were no evidences for LV hypertrophy. In summary, the spectral Doppler showed normal pattern of LV diastolic filling. Normal right

ventricular size and systolic function were detected. Of note, the right atrium was severely dilated, similar to his cousin (patient III:24, family A). Nevertheless, because of the young age of this patient and the remarkable similar phenotype compared with the index patient (III:24), it is expected that the clinical symptoms will potentially increase during the next decades. For that reason, the patient received a pacemaker/implantable cardioverter defibrillator.

In family B (Figure 1B), the index patient (IV:1) had experienced palpitations from an age of 25 years. Clinical workup showed a borderline ARVC phenotype based on nonsustained ventricular tachycardia of left bundle branch block morphology, a positive signal-averaged ECG, and a suspicious family history. Echocardiography and MRI were normal. Review of her father's (III:2) medical history revealed that he had been evaluated in the early 80s because of syncope. Workup had shown frequent PVCs of left bundle branch block morphology. He died suddenly playing golf at the age of 38 years. The probands uncle (III:3) had experienced syncope during running at the age of 38 years and was diagnosed with a nonischemic cardiomyopathy (ejection fraction, 25%) and nonsustained ventricular tachycardia. His ejection fraction improved to 50% on therapy (angiotensin-converting-enzyme inhibitor, β -blocker, digoxin, spironolactone, implantable cardioverter defibrillator), but he developed chronic atrial fibrillation. All 3 individuals (IV:1, III:2, III:3) were tested positive or obligate carriers of the *DES*-p.H326R (c.977A>G) variant. The probands brother (IV:2) was phenotype and genotype negative (current age, 37 years). No clinical or genetic data were available on individuals II:1 and II:2 because they had died >30 years ago. Individual III:5 was diagnosed with a dilated cardiomyopathy and PVCs before experiencing sudden cardiac arrest at the age of 36 years. Individual IV:4 was initially examined at the age of 9 years because of PVCs and nonsustained ventricular tachycardia. Later, her LV was dilated (LV end diastolic diameter, 69 mm) and ejection fraction was at the lowest 25% but improved to 55% with treatment (angiotensin-converting-enzyme inhibitor, β -blocker, amiodarone, PVC ablation, implantable cardioverter defibrillator). Blood was available from individual IV:4, and she did not carry the *DES*-p.H326R variant. None of the patients had signs of peripheral muscular involvement.

Genetic Analysis and Mutation Detection

Genomic DNA was isolated and purified from the affected individuals using the illustra blood genomicPrep Mini Spin Kit (GE Healthcare, Chalfont St Giles, United Kingdom). The BigDye Terminator v1.1 Cycle Sequencing Kit (Applied Biosystems, CA) and an ABI310 Genetic Analyzer (Applied Biosystems, CA) were used for sequencing according to the manufacturer's instructions. The sequences were analyzed with the Variant Reporter Software v1.0 (Applied Biosystems, CA). The allele frequencies of novel variants were determined in 394 healthy control individuals using the TaqMan SNP Genotyping Assay (Applied Biosystems, CA). The consent of all participants was obtained, and the study was approved by the ethics committee.

Cloning and Site-Directed Mutagenesis

The sequence variants were inserted into the plasmids pET100D-Desmin¹² and pEYFP-N1-Desmin²¹ using appropriate primers and the QuickChange Lightning Kit (Agilent Technologies, Santa Clara) according to the manufacturer's instructions (see Table I in the online-only Data Supplement). The *DES* coding regions were verified by sequencing using the BigDye Terminator v1.1 Cycle Sequencing Kit (Applied Biosystems, CA). The reference cDNA of human desmin (NM_001927.3) was used for comparison.

Cell Culture

H9c2, HeLa, C2C12, and SW-13 cells (LGC Standards, Middlesex) were cultured in DMEM (Invitrogen, Carlsbad) supplemented with 10% FCS, 4.5 g/L glucose, and penicillin/streptomycin. The HL-1 cells (kindly provided by Dr William Claycomb) were cultured in Claycomb medium (Sigma-Aldrich, St. Louis) supplemented with 10% FCS, 2 mmol/L L-glutamine, 100 nmol/L

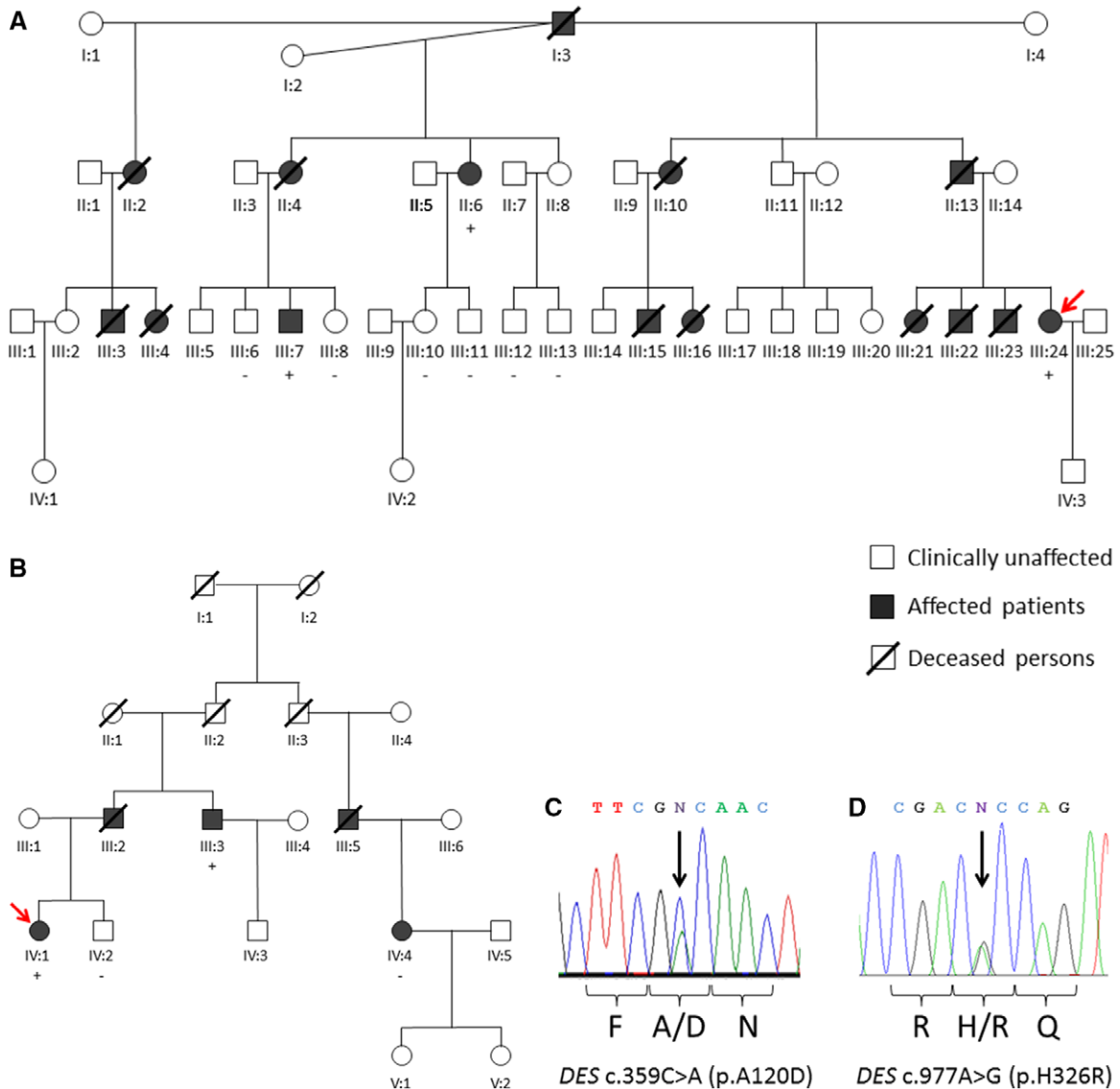


Figure 1. Identification and verification of the *DES* variants. Pedigrees of family A (**A**) and family B (**B**). Squares represent males, and circles represent females. Deceased individuals are indicated by slashes. The index patients are marked by a red arrow. Genotypes are shown by present (+) or by absent (-) of the heterozygous *DES* mutations (p.A120D, family A; p.H326R, family B). Electropherograms showing the heterozygous alleles c.359C>A, p.A120D (**C**) and c.977A>G, p.H326R (**D**). Converted codons lead to the protein changes p.A120D (**C**) and p.H326R (**D**).

norepinephrine, and penicillin/streptomycin.²² Cardiomyocytes derived from human-induced pluripotent stem cells were generated and cultured as previously described.^{23,24} Lipofectamine 2000 (Invitrogen, Carlsbad) was used to transfect the cells according to the manufacturer's protocol.

Immunohistochemistry and Fluorescence Microscopy

Transfected cells were fixed with methanol (15 minutes, -20°C) and were then permeabilized with 0.1% Triton X-100 (20 minutes, room temperature). After blocking with 1% BSA/PBS, the cells were incubated with 7.5 $\mu\text{g}/\text{mL}$ anti-desmin antibodies (R&D Systems, Minneapolis) or 25 $\mu\text{g}/\text{mL}$ anti-vimentin antibodies (Sigma-Aldrich, St. Louis) overnight at 4°C and were gently washed with 1% BSA/PBS. Then the cells were incubated with Cy3-conjugated anti-goat-IgG or anti-mouse-IgG secondary antibodies (1:400, Jackson ImmunoResearch, West Grove, PA) for 1 hour at RT. The nuclei were stained with 1 $\mu\text{g}/\text{mL}$ 4',6-diamidino-2-phenylindole (DAPI, 5 minutes, RT). The cells were washed with

PBS, and fluorescence images were recorded with an Eclipse TE2000-U microscope (Nikon, Tokyo, Japan) equipped with a Digital sight DS-2MV CCD camera (Nikon, Tokyo, Japan), yellow fluorescence protein, Cy3, and DAPI filter sets (AHF, Tübingen, Germany) and an oil immersion objective (Plan Apochromat 60x/1.40 Oil; Nikon, Tokyo, Japan).

The paraffin-embedded sections (5 μm) were deparaffinized and rehydrated with a standard technique using xylene and ethanol. The heart tissue was stained with primary antibodies overnight at 4°C (see Table II in the online-only Data Supplement) and afterward with secondary antibodies for 1 hour at room temperature.

Desmin Expression and Purification

Bacteria (BL21-Star-DE3) transformed with desmin expression constructs (see Table I in the online-only Data Supplement) were cultured in Luria Broth medium supplemented with ampicillin (100 $\mu\text{g}/\text{mL}$). The desmin expression was induced with isopropyl- β -D-1-thiogalactopyranoside (IPTG, 1 mmol/L), when the $A_{600\text{ nm}}$ reached a value of 0.6 to 0.8. After 4-hour incubation at 37°C , bacteria were harvested by centrifugation and were frozen at -80°C . The inclusion

bodies were isolated as earlier described.¹² Finally, the proteins were dissolved (8 mol/L urea, 20 mmol/L Tris-HCl, 100 mmol/L NaH₂PO₄, pH 8.0) and supplied to a HiTrap DEAE Sepharose Fast Flow column (GE Healthcare, Chalfont St Giles, United Kingdom) using the ÄKTApurifier system (GE Healthcare, Chalfont St Giles, United Kingdom). Recombinant desmin was eluted by a linear salt gradient (0–0.35 mol/L NaCl), and fractions were pooled and supplied to 5 mL Ni²⁺-NTA (Qiagen, Hilden, Germany) overnight at 4°C. The column was washed with buffer (8 mol/L urea, 20 mmol/L Tris-HCl, 10 mmol/L imidazole, pH 8.0) until A_{280 nm} decreased to a constant value <0.01. Recombinant desmin molecules were eluted with imidazole-containing buffer (8 mol/L urea, 20 mmol/L Tris-HCl, 300 mmol/L imidazole, pH 6.9). The fractions containing >95% recombinant desmin were pooled and stored at –80°C. The desmin concentration was determined by absorption measurement at 280 nm ($\epsilon=26.300 \text{ (mol/L)}^{-1}\cdot\text{cm}^{-1}$, www.expasy.org).

Proteolysis and Mass Spectrometry

The identity of purified desmin variants was proven by mass spectrometry. The desmin variants (20 μg , 100 mmol/L Tris-HCl, pH 8.5) were incubated with 0.08 mg dithiothreitol (30 minutes, 60°C) and were digested with trypsin or Lys-C (Sigma-Aldrich, St. Louis) according to the manufacturer's instructions. The lyophilized peptides were dissolved in 0.1% formic acid and identified by peptide mass fingerprinting using electrospray ionization-liquid chromatography/mass spectrometry and were confirmed by electrospray ionization-liquid chromatography/tandem mass spectrometry using a micrOTOF-Q hybrid mass spectrometer (Bruker, Bremen, Germany). A Jupiter 5u C18 (2.0 \times 150 mm, 300 Å) reverse phase column was used for chromatography. The spectrometer was run in multiple reactions monitoring mode (20–25 eV) for tandem mass spectrometry analysis.

Atomic Force Microscopy

After a stepwise dialysis into buffer without urea (5 mmol/L Tris-HCl, 1 mmol/L dithiothreitol, pH 8.4), the filament formation of recombinant desmin was initiated by addition of an equal volume of sodium chloride buffer (200 mmol/L NaCl, 45 mmol/L Tris-HCl, pH 7.0) and subsequent heating to 37°C for 1 hour as previously described.²⁵ The assembled desmin species (150 $\mu\text{g}/\text{mL}$) were applied to freshly cleaved mica substrates (Plano, Wetzlar, Germany), rinsed with deionized water to remove unbound desmin, and dried under a gentle flow of nitrogen. Topographical AFM imaging was done with a Multimode AFM and Nanoscope IIIa controller (Bruker, Santa Barbara) as previously described.²¹

Results

Genetic Analysis

We identified 2 unreported heterozygous sequence variants p.A120D (c.359C>A) and p.H326R (c.977A>G) in the *DES* gene (Figure 1C and 1D). Both variants were not present in 394 healthy control individuals. Furthermore, both variants were not present in publicly available databases and in >12500 alleles from the NHLBI Exome Sequencing Project (<http://evs.gs.washington.edu/EVS/>).

The index patient (III:24) of family A (Figure 1A) was tested for mutations in ARVC-related genes *DSG2*, *DSC2*, *JUP*, *PKP2*, *DSP*, *LMNA*, *TMEM43*, *PLN* and in addition by a gene panel including *LDB3/ZASP*, *TNNT2*, *SGCD*, *ACTC1*, *MYH7*, *TPM1*, *TNNI3*, *TAZ*, *TTR*, *MYBC3*, and *LAMP2*, which represent the most frequent dilated cardiomyopathy genes. We identified in the index patient of family A (III:24) the *PKP2* variant (c.1577C>T, p.T526M), which was earlier defined as a nonpathogenic single-nucleotide polymorphism.^{26,27} In the NHLBI Exome Sequencing Project,

the *PKP2* variant (c.1577C>T, p.T526M) was found 48 \times in 12958 alleles (<http://evs.gs.washington.edu/EVS/>), which is by far above the expected prevalence of the mutation if this was relevant for the disease. The Danish index patient (IV:1) of family B (Figure 1B) has also been screened for mutations in above listed ARVC genes without positive findings.

The p.A120D is part of the initial helix motive in coil 1 of the desmin protein and is absolutely conserved in different species (Figure 2A and 2B). This mutation is localized in a b-position of the heptade sequence and therefore in close proximity to N116. The other sequence variant p.H326R is localized at the heptade's f-position in coil 2 of the rod domain (Figure 2B and 2C). However, this amino acid is not completely conserved among IF proteins (Figure 2C), complicating its pathogenic interpretation.

Filament or Aggregate Formation of the Desmin Variants in Transfected Cells

We investigated the filament formation of the different *DES* variants in transfected SW-13, HL-1, H9c2, C2C12, HeLa, and cardiomyocytes derived from human-induced pluripotent stem cells. In these transfection experiments, desmin p.H326R formed in all cell line filaments compared with the WT (Figure 3). In contrast, desmin-p.A120D accumulated into cytoplasmic aggregates independently of the transfected cell line (Figure 3).

We further investigated by immunohistochemistry whether the endogenous IFs were impaired by coexpression of the desmin mutants. These analysis revealed that the expression of desmin-p.A120D influences the assembly of endogenous desmin in the muscle cell lines HL-1, H9c2, and C2C12, indicating a dominant inhibiting defect (Figure 4). Desmin and vimentin form heterofilaments when coexpressed within the same cell.³³ Therefore, we used endogenously vimentin expressing HeLa cells to investigate whether the desmin mutants induce a coaggregation with vimentin. In contrast to desmin-p.H326R and desmin-WT, the p.A120D mutant induced a partially coaggregation with vimentin in transfected HeLa cells. Nevertheless, the vimentin network was not strongly affected by the expression of desmin-p.A120D.

In Vitro Desmin Assembly Using AFM

To get better insights into the putative filament formation defects caused by these new desmin variants, we purified the recombinant desmins by ion exchange and immobilized metal affinity chromatography and analyzed the filament formation in vitro by AFM. In accordance with our cell culture experiments, we found that the variant p.H326R formed filaments similar to WT desmin (Figure 5). In contrast, desmin-p.A120D formed small accumulated fibrils (Figure 5), suggesting severe impairment of the filament elongation step by this mutation.

Investigation of Different Model Mutants at Position A120

Because it is not known whether the loss of the methylene group or the gain of the aspartate residue is causative for aggregation of desmin-p.A120D, we constructed different model variants (p.A120E, p.A120K, p.A120R, p.A120V, and p.A120L) to get more insights into the nature of the amino acid residue, which

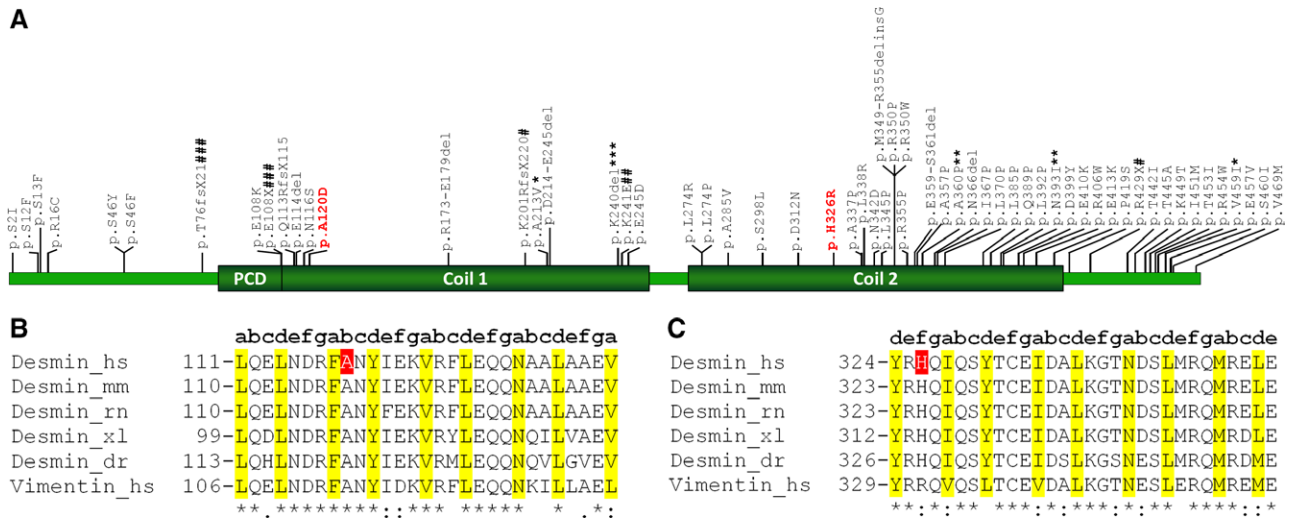


Figure 2. Localization of the identified *DES* mutations within the desmin sequence. **A**, Schematic domain structure of the desmin protein and the distribution of known disease-causing mutations. Some *DES* mutations affecting the splice sites are not shown.^{28,29} *This sequence variants were also identified in healthy control persons.⁹ #p.K201RfsX20 and p.R429X were both identified in the same patient.³⁰ **p.A360P and p.N393I were both identified in the same patients.³ ##In the same patient with arrhythmogenic right ventricular cardiomyopathy, a pathogenic *PKP2* mutation (p.T816RfsX10) was identified.¹⁵ ***The mutation p.K240del was originally described as an insertion mutation.³¹ However, the authors corrected the sequence analysis in 2007. ###Two siblings compound heterozygous for the mutations p.T76fsX21 and p.E108X were described.³² **B** and **C**, Alignment of the desmin/vimentin sequences of *Homo sapiens* (hs), *Mus musculus* (mm), *Rattus norvegicus* (rn), *Xenopus laevis* (xl), and *Danio rerio* (dr). The heptade sequence is highlighted in yellow and the positions of the mutations identified in this article are marked in red.

causes the filament formation defect of desmin-p.A120D. In transfected cells, the hydrophobic model mutants (p.A120V and p.A120L) formed filaments similar to WT desmin (Figure 6). In contrast, the exchange of A120 against positive or negative amino acids induced desmin aggregation, with the exception of p.A120K (Figure 6). In summary, these experiments reveal the essential role of a hydrophobic amino acid at position 120 for the filament formation.

Immunohistochemistry in Cardiac Tissue

Ventricular myocardium of individual II:6 (family A) was available from heart transplantation (Mount Sinai Hospital, Los Angeles). Confirming the in vitro results of the cell culture and AFM experiments with the mutant desmin-p.A120D, we found a high density of desmin aggregates within the ventricular myocardium, which was undetectable in the ventricles of rejected donor hearts (Figure 7).

In addition, when the slices of the *DES*-p.A120D heart were costained for desmoplakin, colocalization of desmin and desmoplakin could not be observed. Thus, desmin was

detectable in the *DES*-p.A120D heart of the mutation carrier in the z-bands and in prominent protein aggregates but not within the ID (Figure 7).

Recently, remodeling for plakoglobin (*JUP*)³⁴ as well as connexin-43 (*Cx43*)³⁵ was described in patients with arrhythmogenic cardiomyopathy. Therefore, we investigated whether the localization of both proteins were affected in the patient with the *DES*-p.A120D mutation. These results demonstrate that plakoglobin as well as connexin-43 are localized in the ID similar as in healthy control persons (Figures II and III in the online-only Data Supplement).

Discussion

At the end of the 1990s, the first mutations in the human *DES* gene were published.^{3,4} It became obvious that mutations within the *DES* gene may lead to skeletal and cardiac myopathies with a broad spectrum of pathological muscle phenotypes even within the same family.³⁶ Of note, ~74% of the patients with desminopathy develop a cardiac phenotype such as conduction disease, arrhythmias, or cardiomyopathies.⁶ Nevertheless,

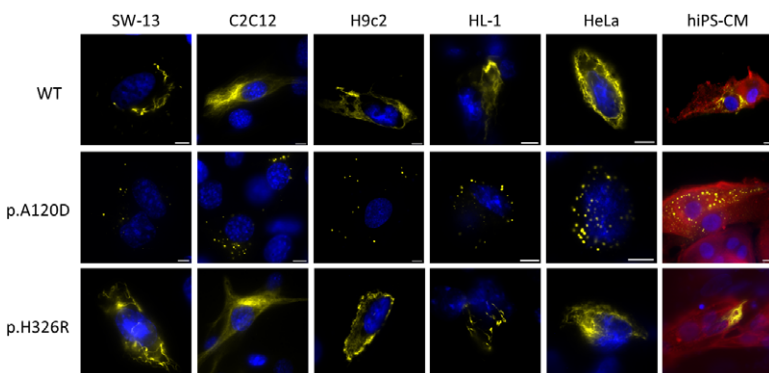


Figure 3. Impairment of filament formation by desmin mutants in transfected cells. Representative fluorescence images of transfected SW-13, H9c2, HL-1, C2C12, and HeLa cells and cardiomyocytes derived from human-induced pluripotent stem cells (hiPS-CM) expressing desmin-eYFP constructs (hiPS-CM were identified by staining for sarcomeric α -actinin using Alexa Fluor 555-conjugated secondary antibodies (red). Nuclei were stained with DAPI (blue). Scale bars represent 10 μ m. WT indicates wild type; and YFP, yellow fluorescence protein.

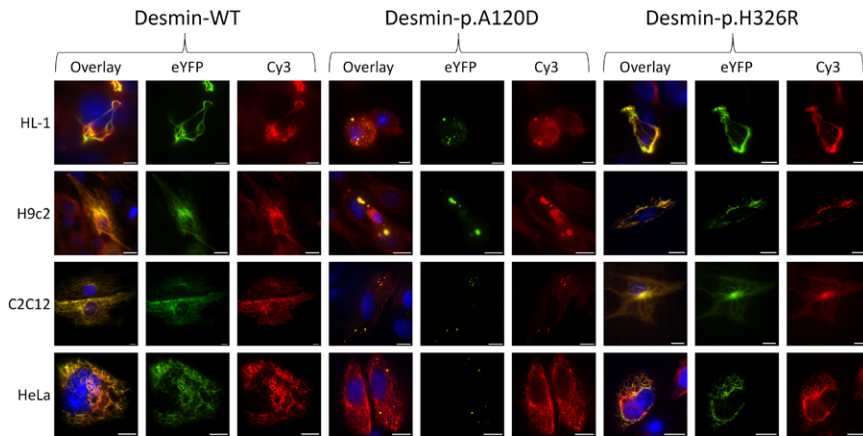


Figure 4. Endogenously expressed intermediate filament proteins in cells transfected with desmin mutants. Representative fluorescence images of transfected HL-1, H9c2, C2C12, and HeLa cells expressing desmin-eYFP constructs (green), immunostained for desmin (HL-1, H9c2, and C2C12) or vimentin (HeLa) using Cy3-conjugated secondary antibodies (red). The nuclei were stained with DAPI (blue). Scale bars represent 10 μm . WT indicates wild type; and YFP, yellow fluorescence protein.

the molecular pathomechanisms leading to desmin-related arrhythmogenic cardiomyopathies are not well understood.

In recent years, mutations of *DES* associated with an ARVC-related phenotype were found.^{10–15} In this study, we identified and characterized the 2 novel heterozygous *DES* variants p.A120D and p.H326R.

The variant p.A120D is localized within the highly conserved IF consensus motif at the N-terminal segment of coil 1. The amino acid residue A120 is absolutely conserved in different human IF proteins and among species.³⁷ Even lamin of *Hydra attenuata* contains this amino acid.^{38,39} Interestingly, mutations in the homologous positions of the genes coding for keratins K5,^{40,41} K10,⁴² K12,⁴³ K86,⁴⁴ and lamin A/C⁴⁵ cause severe clinical diseases of eye, skin, and muscle, respectively. The desmin variant p.A120D was not detectable in 788 control chromosomes and revealed a severe filament formation defect in cell culture and AFM. These data were confirmed by immunostaining of the failing ventricular myocardium of the affected patient. Interestingly, the desmin staining within the ID was undetectable in the mutation carrier. It is known that desmin is linked to the cardiac desmosome via the plaque protein desmoplakin.⁴⁶ Based on yeast 2 hybrid analyses, this protein interaction was claimed to be affected by the desmin mutant

p.I451M.⁴⁶ However, the transgenic murine model of Mavroidis et al⁴⁷ revealed in contrast that this mutation affects the positioning of desmin to the z-bands but not in the ID. Thus, it remains an open question whether a specific (sub-)domain of desmin is linked to the ID via desmoplakin. The lack of desmin within the ID might explain the high prevalence of malignant arrhythmias in the affected family A. Of note, the pedigree of this family reveals several SCDs among teenaged family members, which might reflect the arrhythmogenic potential of desmin-p.A120D. Recently, remodeling of plakoglobin and connexin-43 were described in arrhythmogenic cardiomyopathy patients.^{34,35} Nevertheless, plakoglobin staining as well as connexin-43 remodeling are controversially discussed in the literature because the absence could not be detected in every patient.^{48–51} In this study, we demonstrate comparable amounts of plakoglobin and connexin-43 within the ID in heart tissue of a healthy control person and of a patient with the *DES*-p.A120D mutation. Based on these experiments, we conclude that the remodeling of plakoglobin and connexin-43 does not play a major role for the pathomechanisms caused by this specific *DES* mutation.

The mutation p.A120D leads to an exchange of a hydrophobic amino acid side chain against an acidic one. We hypothesized that a hydrophobic amino acid at position 120 is essential

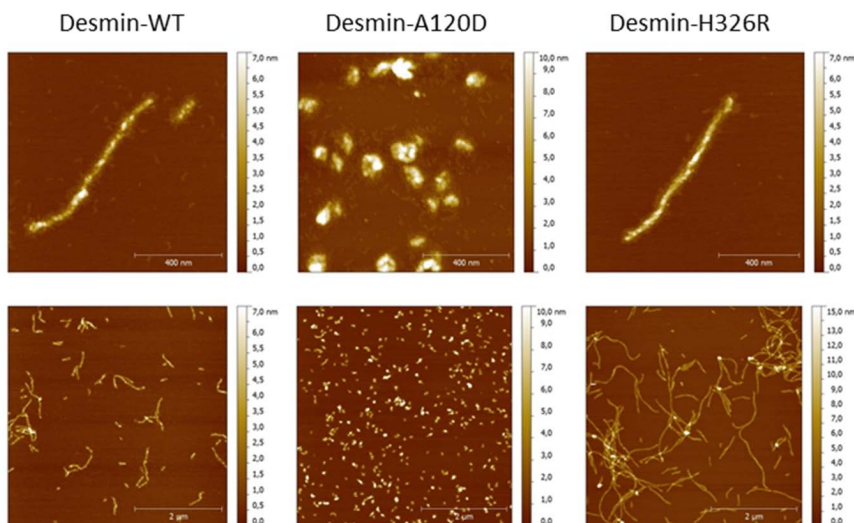


Figure 5. Filament formation of recombinant mutant desmin. Desmin was expressed in *Escherichia Coli*, purified, prepared on mica, and measured under ambient conditions in atomic force microscopy (AFM) tapping mode of operation. Representative AFM topography images of desmin-WT, desmin-p.A120D, and desmin-p.H326R are shown from left to right in (1 \times 1 μm) AFM scans (top) and (5 \times 5 μm) AFM scans (bottom). Distinct filament structures could be discerned for desmin-wt and desmin-p.H326R with typical (averaged) dimensions of 500 nm (length), 30 nm (width), and 3 to 6 nm (height). The apparent width of 30 nm is consistent with a real filament diameter of 8 to 10 nm that is broadened by artifacts attributable to a finite AFM tip radius of \approx 20 nm. The reduced height is attributed to surface capillary force effects. In contrast, desmin-p.A120D exhibited complete loss of

filament structure, presenting more globular structures with typical size of 85 nm. Representative AFM topography images are shown. WT indicates wild type.

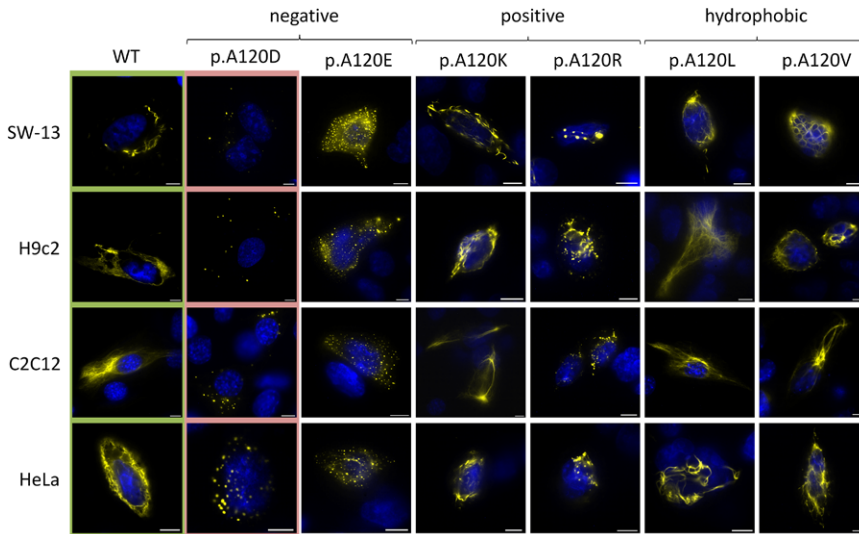


Figure 6. Analysis of model mutants for desmin-p.A120D in different cell lines. Representative fluorescence images of transfected SW-13, H9c2, C2C12, and HeLa cells expressing indicated mutant desmin-eYFP constructs (yellow). Nuclei were stained with DAPI (blue). Scale bars represent 10 μm. WT indicates wild type; and YFP, yellow fluorescence protein.

for filament formation. For testing this hypothesis, we constructed further model mutants with (1) hydrophobic residues (p.A120L and p.A120V), (2) negative (p.A120E), and (3) positive charge (p.A120R and p.A120K). Remarkably, ionic side chains at this position disturbed the filament formation with the exception of the lysine residue, whereas the experiments with hydrophobic amino acid side chains reveal that even a larger mutant amino acid at this position does not disturb filament formation. We conclude from these data that a steric hindrance of the side chain can be excluded as a reason for the p.A120D filament formation defect. We assume that this position within the

desmin primary structure, which is in the neighborhood of the recently published mutations p.N116S¹² and p.E114del,¹³ might be a hotspot for desminopathies associated with arrhythmias. It could be speculated that the intramolecular interaction of this part of the desmin coil 1 with its head domain might be affected, which was recently shown for vimentin.^{52,53}

In summary, although a cosegregation analysis was not possible in family A because of the lack of genomic DNA from suddenly deceased members, we conclude from our experiments that *DES*-p.A120D is indeed a disease-causing mutation with a high potential for SCD.

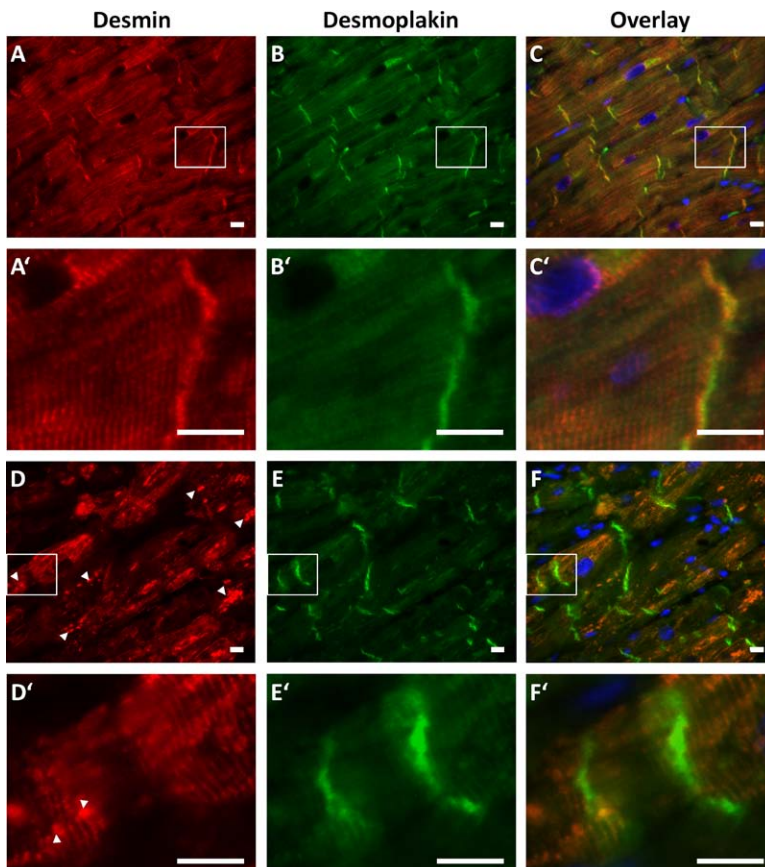


Figure 7. Immunohistological analysis of cardiac tissue heterozygous for the *DES*-p.A120D mutation. **A to C**, Representative fluorescence images of a control sample from a human nonfailing control heart showing normal localization of desmin (red) and desmoplakin (green) at the intercalated disks (IDs) and at the z-bands. **D to F**, Representative paraffin sections of cardiac tissue of patient II:6 demonstrate strong accumulation of desmin (white arrowheads). Of note, the desmin localization is completely lost at the ID. Scale bars represent 10 μm.

The amino acid p.H326 is conserved among vertebrate desmins. However, arginine at this position is also found in the human homolog vimentin. In addition, this allele was not found in 788 control chromosomes or in the Washington Exome Data. To assess the pathogenic potential of this variant, we investigated *in vitro* the influence of p.H326R on filament formation and performed a cosegregation analysis within the family. When tested in cell culture experiments, this recombinant desmin variant did not reveal any filament formation defect, which was also supported by AFM of the purified recombinant desmin. Nevertheless, we cannot exclude that other relevant functions of desmin, such as biomechanical properties or protein–protein interactions, that is, with desmoplakin, might be disturbed by this variant. Of note, the variant did not completely cosegregate within family B. In summary, we regard p.H326R as a rare variant of unknown pathogenic significance.

Acknowledgments

We thank all participating patients. We are grateful to Birte Bohms for excellent technical assistance. Furthermore, we thank Dr Dawn Lombardo (University of Irvine) for her help in clinical investigations. In addition, we thank Dr Bianca Werner (Heart and Diabetes Centre NRW, Germany) for providing the HeLa cells, Dr Christine Mummery (Leiden University Medical Centre, The Netherlands) for providing the END2 cells, and Dr William Claycomb (New Orleans) for providing the HL-1 cells.

Sources of Funding

Dr Milting was kindly funded by the Erich and Hanna Klessmann Foundation, Gütersloh, Germany, and by FoRUM grant (F649-2009) of the Ruhr-University Bochum. This work was also supported by the grant from the *Bundeministerium für Bildung und Forschung* (BMBF) to T. Šaric (grant No.: 01 GN 0824). J.H. Svendsen was funded by The Danish National Research Foundation, The John and Birthe Meyer Foundation, The Research Foundation of the Heart Centre, Copenhagen University Hospital, and The Arvid Nilsson Foundation.

Disclosures

None.

Appendix

From the Erich and Hanna Klessmann Institute for Cardiovascular Research and Development (EHKI), Heart and Diabetes Center NRW, Ruhr-University Bochum, Bad Oeynhausen, Germany (A.B., B.K., T.S., R.C., D.G., U.S., J.G., H.M.); Experimental Biophysics and Applied Nanoscience, Faculty of Physics, Bielefeld Institute for Biophysics and Nanoscience (BINAS), Bielefeld University, Bielefeld, Germany (M.D., V.W., K.T., D.A.); Division of Genetics and Metabolism, Department of Pediatrics, University of California, Irvine (E.D., S.M., J.G., V.K.); Division of Human Genetics, Department of Pediatrics, Cincinnati Children's Hospital, OH (T.H.); Institute for Neurophysiology, Medical Center, University of Cologne, Cologne, Germany (A.F., T.Š.); Physikalisch-Technische Bundesanstalt (PTB), Braunschweig, Germany (H.C.); Department of Cardiology, Rigshospitalet, Copenhagen University Hospital, Copenhagen, Denmark (J.H.S., M.S.O., A.H.C.); and The Danish National Research Foundation Centre for Cardiac Arrhythmia, Copenhagen, Denmark (J.H.S., M.S.O., A.H.C.).

References

- Potschka M, Nave R, Weber K, Geisler N. The two coiled coils in the isolated rod domain of the intermediate filament protein desmin are staggered. A hydrodynamic analysis of tetramers and dimers. *Eur J Biochem*. 1990;190:503–508.
- Herrmann H, Strelkov SV, Burkhard P, Aebi U. Intermediate filaments: primary determinants of cell architecture and plasticity. *J Clin Invest*. 2009;119:1772–1783.
- Goldfarb LG, Park KY, Cervenáková L, Gorokhova S, Lee HS, Vasconcelos O, et al. Missense mutations in desmin associated with familial cardiac and skeletal myopathy. *Nat Genet*. 1998;19:402–403.
- Muñoz-Mármol AM, Strasser G, Isamat M, Coulombe PA, Yang Y, Roca X, et al. A dysfunctional desmin mutation in a patient with severe generalized myopathy. *Proc Natl Acad Sci U S A*. 1998;95:11312–11317.
- Li D, Tapscott T, Gonzalez O, Burch PE, Quiñones MA, Zoghbi WA, et al. Desmin mutation responsible for idiopathic dilated cardiomyopathy. *Circulation*. 1999;100:461–464.
- van Spaendonck-Zwarts KY, van Hessem L, Jongbloed JD, de Walle HE, Capetanaki Y, van der Kooij AJ, et al. Desmin-related myopathy. *Clin Genet*. 2011;80:354–366.
- Cao L, Hong D, Zhu M, Li X, Wan H, Hong K. A novel heterozygous deletion-insertion mutation in the desmin gene causes complete atrioventricular block and mild myopathy. *Clin Neuropathol*. 2013;32:9–15.
- Bär H, Mücke N, Kostareva A, Sjöberg G, Aebi U, Herrmann H. Severe muscle disease-causing desmin mutations interfere with *in vitro* filament assembly at distinct stages. *Proc Natl Acad Sci U S A*. 2005;102:15099–15104.
- Kostareva A, Sjöberg G, Gudkova A, Smolina N, Semernin E, Shlyakhto E, et al. Desmin A213V substitution represents a rare polymorphism but not a mutation and is more prevalent in patients with heart dilation of various origins. *Acta Myol*. 2011;30:42–45.
- van Tintelen JP, Van Gelder IC, Asimaki A, Suurmeijer AJ, Wiesfeld AC, Jongbloed JD, et al. Severe cardiac phenotype with right ventricular predominance in a large cohort of patients with a single missense mutation in the DES gene. *Heart Rhythm*. 2009;6:1574–1583.
- Otten E, Asimaki A, Maass A, van Langen IM, van der Wal A, de Jonge N, et al. Desmin mutations as a cause of right ventricular heart failure affect the intercalated disks. *Heart Rhythm*. 2010;7:1058–1064.
- Klauke B, Kossmann S, Gaertner A, Brand K, Stork I, Brodehl A, et al. De novo desmin-mutation N116S is associated with arrhythmogenic right ventricular cardiomyopathy. *Hum Mol Genet*. 2010;19:4595–4607.
- Vernengo L, Chourbagi O, Panuncio A, Liliënbaum A, Batonnet-Pichon S, Bruston F, et al. Desmin myopathy with severe cardiomyopathy in a Uruguayan family due to a codon deletion in a new location within the desmin 1A rod domain. *Neuromuscul Disord*. 2010;20:178–187.
- Hedberg C, Melberg A, Kuhl A, Jenne D, Oldfors A. Autosomal dominant myofibrillar myopathy with arrhythmogenic right ventricular cardiomyopathy 7 is caused by a DES mutation. *Eur J Hum Genet*. 2012;20:984–985.
- Lorenzon A, Beffagna G, Baucé B, De Bortoli M, Li Mura IE, Calore M, et al. Desmin mutations and arrhythmogenic right ventricular cardiomyopathy. *Am J Cardiol*. 2013;111:400–405.
- Azaouagh A, Churzidse S, Konorza T, Erbel R. Arrhythmogenic right ventricular cardiomyopathy/dysplasia: a review and update. *Clin Res Cardiol*. 2011;100:383–394.
- Gerull B, Heuser A, Wichter T, Paul M, Basson CT, McDermott DA, et al. Mutations in the desmosomal protein plakophilin-2 are common in arrhythmogenic right ventricular cardiomyopathy. *Nat Genet*. 2004;36:1162–1164.
- Heuser A, Plovie ER, Ellinor PT, Grossmann KS, Shin JT, Wichter T, et al. Mutant desmocollin-2 causes arrhythmogenic right ventricular cardiomyopathy. *Am J Hum Genet*. 2006;79:1081–1088.
- Gerull B, Kirchner F, Chong JX, Tagoe J, Chandrasekharan K, Strohm O, et al. Homozygous founder mutation in desmocollin-2 (DSC2) causes arrhythmogenic cardiomyopathy in the Hutterite population. *Circ Cardiovasc Genet*. 2013;6:327–336.
- Elliott P, O'Mahony C, Syrris P, Evans A, Rivera Sorensen C, Sheppard MN, et al. Prevalence of desmosomal protein gene mutations in patients with dilated cardiomyopathy. *Circ Cardiovasc Genet*. 2010;3:314–322.
- Brodehl A, Dieding M, Cakar H, Klauke B, Walhorn V, Gummert J, et al. Functional characterization of desmin mutant p.P419S. *Eur J Hum Genet*. 2013;21:589–590.
- Claycomb WC, Lanson NA Jr, Stallworth BS, Egeland DB, Delcarpio JB, Bahinski A, et al. HL-1 cells: a cardiac muscle cell line that contracts and retains phenotypic characteristics of the adult cardiomyocyte. *Proc Natl Acad Sci U S A*. 1998;95:2979–2984.
- Brodehl A, Hedde PN, Dieding M, Fatima A, Walhorn V, Gayda S, et al. Dual color photoactivation localization

- microscopy of cardiomyopathy-associated desmin mutants. *J Biol Chem*. 2012;287:16047–16057.
24. Fatima A, Xu G, Shao K, Papadopoulos S, Lehmann M, Arnáiz-Cot JJ, et al. *In vitro* modeling of ryanodine receptor 2 dysfunction using human induced pluripotent stem cells. *Cell Physiol Biochem*. 2011;28:579–592.
 25. Kreplak L, Bär H, Leterrier JF, Herrmann H, Aebi U. Exploring the mechanical behavior of single intermediate filaments. *J Mol Biol*. 2005;354:569–577.
 26. Quarta G, Muir A, Pantazis A, Syrris P, Gehmlich K, Garcia-Pavia P, et al. Familial evaluation in arrhythmogenic right ventricular cardiomyopathy: impact of genetics and revised task force criteria. *Circulation*. 2011;123:2701–2709.
 27. den Haan AD, Tan BY, Zikusoka MN, Lladó LI, Jain R, Daly A, et al. Comprehensive desmosome mutation analysis in north americans with arrhythmogenic right ventricular dysplasia/cardiomyopathy. *Circ Cardiovasc Genet*. 2009;2:428–435.
 28. Cetin N, Balci-Hayta B, Gundesli H, Korkusuz P, Purali N, Talim B, et al. A novel desmin mutation leading to autosomal recessive limb-girdle muscular dystrophy: distinct histopathological outcomes compared with desminopathies. *J Med Genet*. 2013;50:437–443.
 29. McDonald KK, Stajich J, Blach C, Ashley-Koch AE, Hauser MA. Exome analysis of two limb-girdle muscular dystrophy families: mutations identified and challenges encountered. *PLoS One*. 2012;7:e48864.
 30. McLaughlin HM, Kelly MA, Hawley PP, Darras BT, Funke B, Picker J. Compound heterozygosity of predicted loss-of-function DES variants in a family with recessive desminopathy. *BMC Med Genet*. 2013;14:68.
 31. Schröder R, Goudeau B, Simon MC, Fischer D, Eggermann T, Clemen CS, et al. On noxious desmin: functional effects of a novel heterozygous desmin insertion mutation on the extrasarcomeric desmin cytoskeleton and mitochondria. *Hum Mol Genet*. 2003;12:657–669.
 32. Henderson M, De Waele L, Hudson J, Eagle M, Sewry C, Marsh J, et al. Recessive desmin-null muscular dystrophy with central nuclei and mitochondrial abnormalities. *Acta Neuropathol*. 2013;125:917–919.
 33. Traub P, Kühn S, Grüb S. Separation and characterization of homo and hetero-oligomers of the intermediate filament proteins desmin and vimentin. *J Mol Biol*. 1993;230:837–856.
 34. Asimaki A, Tandri H, Huang H, Halushka MK, Gautam S, Basso C, et al. A new diagnostic test for arrhythmogenic right ventricular cardiomyopathy. *N Engl J Med*. 2009;360:1075–1084.
 35. Saffitz JE. Arrhythmogenic cardiomyopathy and abnormalities of cell-to-cell coupling. *Heart Rhythm*. 2009;6(8 suppl):S62–S65.
 36. Bergman JE, Veenstra-Knol HE, van Essen AJ, van Ravenswaaij CM, den Dunnen WF, van den Wijngaard A, et al. Two related Dutch families with a clinically variable presentation of cardioskeletal myopathy caused by a novel S13F mutation in the desmin gene. *Eur J Med Genet*. 2007;50:355–366.
 37. Kapinos LE, Schumacher J, Mücke N, Machaidze G, Burkhard P, Aebi U, et al. Characterization of the head-to-tail overlap complexes formed by human lamin A, B1 and B2 “half-minilamin” dimers. *J Mol Biol*. 2010;396:719–731.
 38. Erber A, Riemer D, Hofemeister H, Bovenschulte M, Sticker R, Panopoulou G, et al. Characterization of the Hydra lamin and its gene: a molecular phylogeny of metazoan lamins. *J Mol Evol*. 1999;49:260–271.
 39. Herrmann H, Strelkov SV. History and phylogeny of intermediate filaments: now in insects. *BMC Biol*. 2011;9:16.
 40. Bolling MC, Lemmink HH, Jansen GH, Jonkman MF. Mutations in KRT5 and KRT14 cause epidermolysis bullosa simplex in 75% of the patients. *Br J Dermatol*. 2011;164:637–644.
 41. Hamada T, Kawano Y, Szczecinska W, Wozniak K, Yasumoto S, Kowalewski C, et al. Novel keratin 5 and 14 gene mutations in patients with epidermolysis bullosa simplex from Poland. *Arch Dermatol Res*. 2005;296:577–579.
 42. Yang JM, Yoneda K, Morita E, Imamura S, Nam K, Lee ES, et al. An alanine to proline mutation in the 1A rod domain of the keratin 10 chain in epidermolytic hyperkeratosis. *J Invest Dermatol*. 1997;109:692–694.
 43. Takahashi K, Takahashi K, Murakami A, Okisaka S, Kimura T, Kanai A. Heterozygous Ala137Pro mutation in keratin 12 gene found in Japanese with Meesmann’s corneal dystrophy. *Jpn J Ophthalmol*. 2002;46:673–674.
 44. Winter H, Vabres P, Larrègue M, Rogers MA, Schweizer J. A novel missense mutation, A118E, in the helix initiation motif of the type II hair cortex keratin hHb6, causing monilethrix. *Hum Hered*. 2000;50:322–324.
 45. Brown CA, Lanning RW, McKinney KQ, Salvino AR, Cherniske E, Crowe CA, et al. Novel and recurrent mutations in lamin A/C in patients with Emery-Dreifuss muscular dystrophy. *Am J Med Genet*. 2001;102:359–367.
 46. Lapouge K, Fontao L, Champlaud MF, Jaunin F, Frias MA, Favre B, et al. New insights into the molecular basis of desmoplakin- and desmin-related cardiomyopathies. *J Cell Sci*. 2006;119(pt 23):4974–4985.
 47. Mavroidis M, Panagopoulou P, Kostavasili I, Weisleder N, Capetanaki Y. A missense mutation in desmin tail domain linked to human dilated cardiomyopathy promotes cleavage of the head domain and abolishes its Z-disc localization. *FASEB J*. 2008;22:3318–3327.
 48. Arbustini E, Pasotti M, Pilotto A, Pellegrini C, Grasso M, Previtali S, et al. Desmin accumulation restrictive cardiomyopathy and atrioventricular block associated with desmin gene defects. *Eur J Heart Fail*. 2006;8:477–483.
 49. Basso C, Pilichou K, Thiene G. Is it time for plakoglobin immunohistochemical diagnostic test for arrhythmogenic cardiomyopathy in the routine pathology practice? *Cardiovasc Pathol*. 2013;22:312–313.
 50. Tavora F, Zhang M, Cresswell N, Li L, Fowler D, Franco M, et al. Quantitative Immunohistochemistry of Desmosomal Proteins (Plakoglobin, Desmoplakin and Plakophilin), Connexin-43, and N-cadherin in Arrhythmogenic Cardiomyopathy: An Autopsy Study. *Open Cardiovasc Med J*. 2013;7:28–35.
 51. Paul M, Wichter T, Gerss J, Arps V, Schulze-Bahr E, Robenek H, et al. Connexin expression patterns in arrhythmogenic right ventricular cardiomyopathy. *Am J Cardiol*. 2013;111:1488–1495.
 52. Aziz A, Hess JF, Budamagunta MS, Voss JC, Fitzgerald PG. Site-directed spin labeling and electron paramagnetic resonance determination of vimentin head domain structure. *J Biol Chem*. 2010;285:15278–15285.
 53. Hess JF, Budamagunta MS, FitzGerald PG, Voss JC. Characterization of structural changes in vimentin bearing an epidermolysis bullosa simplex-like mutation using site-directed spin labeling and electron paramagnetic resonance. *J Biol Chem*. 2005;280:2141–2146.

CLINICAL PERSPECTIVE

Mutations in the gene *DES* might cause skeletal and cardiac myopathies including dilated, hypertrophic, restrictive, and arrhythmogenic cardiomyopathy (arrhythmogenic right ventricular cardiomyopathy). Currently, the desmin-specific pathomechanisms leading to the different phenotypes are unknown. Here, we present a novel disease-causing heterozygous *DES* missense mutation (p.A120D) which is clinically associated with dilated atria, arrhythmias, and sudden cardiac death at young age. In addition, we identified a *DES* variant of unknown significance in patients with arrhythmogenic cardiomyopathy (p.H326R). The results of our study indicate that the phenotypes caused by *DES* mutations could be more diverse and partially overlapping between the different cardiomyopathies which should be considered in genetic counseling. Here, we focus on the molecular characterization of desmin p.A120D which causes a severe filament formation defect *in vitro*. Furthermore, we provide evidences that this missense mutation also causes strong desmin aggregation in the myocardium of the affected patients and leads to the loss of desmin staining within the intercalated disk. The absence of desmin at the intercalated disk might contribute to the arrhythmogenic potential of this mutation. In summary, the presented cell culture experiments and the analysis using atomic force microscopy could help to prove the pathogenicity of further desmin variants. These experimental methods could assist to identify the pathogenic impact of *DES* mutations. This might contribute to risk assessment and genetic counseling of families with desminopathies in the future.